Accepted Manuscript

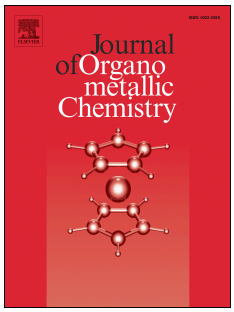

Syntheses, structures and catalytic activities of two cyclopalladated complexes derived from *N'*-(2-naphthaldimine)benzohydrazide

G. Narendra Babu, A.R. Balavardhana Rao, Srinivas Keesara, Samudranil Pal

PII: S0022-328X(17)30482-5

DOI: 10.1016/j.jorganchem.2017.08.002

Reference: JOM 20055

To appear in: *Journal of Organometallic Chemistry*

Received Date: 31 May 2017

Revised Date: 2 August 2017

Accepted Date: 3 August 2017

Please cite this article as: G.N. Babu, A.R.B. Rao, S. Keesara, S. Pal, Syntheses, structures and catalytic activities of two cyclopalladated complexes derived from *N'*-(2-naphthaldimine)benzohydrazide, *Journal of Organometallic Chemistry* (2017), doi: 10.1016/j.jorganchem.2017.08.002.

Graphical Abstract

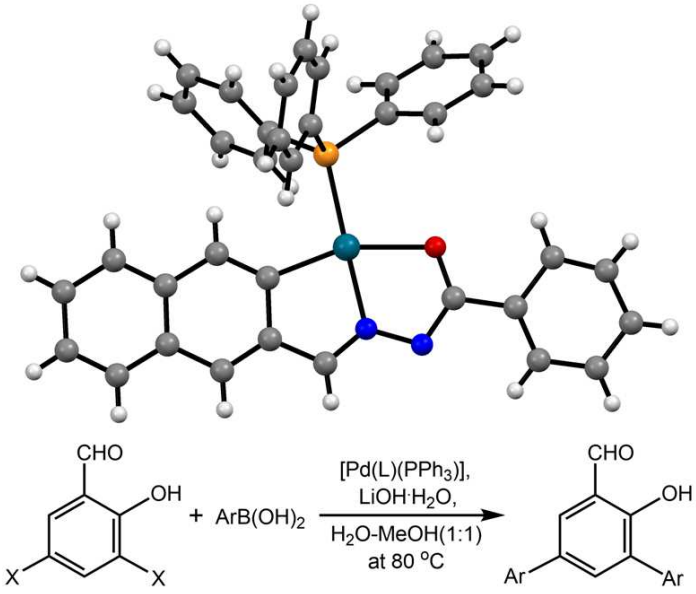

Syntheses, structures and catalytic activities of two cyclopalladated complexes derived from *N′*-(2-naphthaldimine)benzohydrazide

G. Narendra Babu, A. R. Balavardhana Rao, Srinivas Keesara, Samudranil Pal*

School of Chemistry, University of Hyderabad, Hyderabad 500 046, India

ABSTRACT

Condensation reaction of 2-naphthaldehyde with one equivalent of benzohydrazide in presence of acetic acid in refluxing methanol yielded the Schiff base *N′*-(2-naphthaldimine)benzohydrazide (H_2L) in 86% yield. Reaction of equimolar amounts of Li_2PdCl_4 (generated in situ from $PdCl_2$ and LiCl taken in 1:2 mole ratio), H_2L and $NaOAc{\cdot}3H_2O$ in methanol at room temperature provided the complex [Pd(HL)Cl] (**1**) in 82% yield. Treatment of one mole equivalent of **1** with two mole equivalents of PPh_3 in acetone at room temperature produced the complex [Pd(L)(PPh_3)] (**2**) in 72% yield. The Schiff base and the two complexes were characterized by elemental analysis, mass spectrometric and various spectroscopic (IR, UV-Vis and ^{1}H-NMR) measurements. The molecular structures of both complexes (**1** and **2**) were determined by single crystal X-ray crystallography. In each square-planar complex, the tridentate ligand (HL^- in **1** and L^{2-} in **2**) acts as pincer-like CNO-donor. The fourth coordination site is occupied by chloride in **1**, while that in **2** is satisfied by the P-atom of PPh_3. The 2-naphthyl fragment of both HL^- and L^{2-} is palladated at the 3-position. Complex **2** was found to be an effective catalyst for one-pot Suzuki-Miyaura double cross-coupling reactions of 3,5-dihalosalicylaldehydes with a variety of arylboronic acids to provide the corresponding triaryl products in moderate to excellent yields.

Keywords: Cyclopalladation; Regioselective; *N′*-(2-naphthaldimine)benzohydrazide; Crystal structures; Spectroscopic properties; Double cross-coupling

1. Introduction

Syntheses of new cyclometallated complexes continue to attract immense interest because of the potential applications of such species in a diverse range of research areas that include materials science, biological studies, pharmaceutical chemistry and organic synthesis [1–10]. We have been working on cyclometallated platinum group metal ion complexes with a variety of Schiff bases prepared by condensation reactions of mono- or polycyclic aromatic aldehydes with aroylhydrazides, thiosemicarbazides and thioaroylhydrazides during the past several years [11–20]. In all these complexes, the ligands have the pincer like CNO- or CNS-coordination mode. Based on the position of the azomethine group, the Schiff bases derived

* Corresponding author.
E-mail address: spal@uohyd.ac.in (S. Pal)

from polycyclic aromatic aldehydes may provide the prospect for cyclometallation of the polycyclic moiety in a regioselective way and isolation of the corresponding cyclometallates [13–18]. Regioselective cyclometallation reaction is an important tool in organic synthesis reactions as it can assist in functionalization of a specific site among several available. The Schiff base *N'*-(2-naphthaldimine)benzohydrazide (H_2L, 2 Hs represent the amide-H and the H-atom at the 1- or 3-position of the 2-naphthyl group) is one such Schiff base. It is expected that the chelation of the Schiff base via the azomethine-N and the amide-O atom will bring the 2-naphthyl moiety in close proximity of the metal center for the activation of its C–H bond either at the 1- or 3-position both being *ortho* to the azomethine group and eventual cyclometallation at one of the two C-atoms. In the present work, we have studied the palladium(II) coordination chemistry of H_2L to examine how the cyclopalladation of the 2-naphthyl fragment occurs. In this effort, we have isolated two complexes, [Pd(HL)Cl] (**1**) and [Pd(L)(PPh_3)] (**2**), in which the 3-position of the 2-naphthyl fragment of each of the two pincer-like tridentate ligands (HL^- and L^{2-}) is regioselectively metallated (Scheme 1). In the following account, we report the syntheses, X-ray crystal structures and spectroscopic properties of these two complexes. The catalytic activities of both complexes in the one-pot Suzuki-Miyaura double cross-coupling reactions of 3,5-dihalosalicylaldehydes with various arylboronic acids have been also evaluated.

2. Experimental

2.1. Materials

All chemicals used in this work were of analytical grade available commercially and were used as received without any further purification. All solvents used were purified by standard procedures [21].

2.2. Physical measurement

Elemental (CHN) analysis measurements were performed using a Thermo Finnigan Flash EA1112 series elemental analyzer. High resolution mass spectra were recorded with a Bruker Maxis (ESI-TOF analyzer) spectrometer. A Sherwood Scientific balance was used for room temperature magnetic susceptibility measurements. The solution electrical conductivities were measured with the help of a Digisun DI-909 conductivity meter. A Thermo Scientific Nicolet 380 FT-IR spectrophotometer was used to collect the infrared spectra. The electronic absorption spectra were recorded by employing a Shimadzu UV3600

UV-Vis-NIR spectrophotometer. A Bruker spectrometer was used to record the ^{1}H (400 MHz, $SiMe_4$ as an internal standard) and $^{31}P\{^{1}H\}$ (160 MHz, 85% H_3PO_4 as an external standard) NMR spectra.

2.3. Synthesis of H_2L

Few drops of acetic acid were added to a methanol solution (40 ml) of benzohydrazide (681 mg, 5 mmol) and 2-naphthaldehyde (786 mg, 5 mmol) and the resulting mixture was boiled under reflux for 5 h. The reaction mixture was then cooled to room temperature. The white solid precipitated was filtered, washed with methanol (2 x 15 ml) and finally dried in vacuum. Yield: 1.18 gm (86%). Anal. Calcd for $C_{18}H_{14}N_2O$ (%): C, 78.81; H, 5.14; N, 10.21. Found (%): C, 78.65; H, 5.21; N, 10.12. HRMS in $CHCl_3$ m/z found (calcd) for $[M+H]^+$: 275.1187 (275.1184). Selected IR bands: ν (cm^{-1}) = 3199 (N–H), 1638 (C=O), 1605 (C=N). UV-Vis in Me_2NCHO: λ_{max} (nm) (ε (10^4 M^{-1} cm^{-1})) = 347^{sh} (0.65), 333^{sh} (1.74), 315 (2.48), 282 (2.01), 274 (1.86). ^{1}H NMR in $(CD_3)_2SO$: δ (ppm) = 11.99 (s, 1H), 8.64 (s, 1H), 8.16 (s, 1H), 8.03–7.93 (m, 6H), 7.63–7.53 (m, 5H).

*2.4. Synthesis of [Pd(HL)Cl] (**1**)*

To a methanol (30 ml) solution of $Li_2[PdCl_4]$ (generated in situ from $PdCl_2$ (178 mg, 1 mmol) and LiCl (85 mg, 2 mmol)) were added H_2L (275 mg, 1 mmol) and $NaOAc{\cdot}3H_2O$ (137 mg, 1 mmol) and the mixture was stirred at room temperature (298 K) for 24 h. The yellow solid separated was collected by filtration, washed with methanol (2 x 10 ml) and then dried in vacuum. Yield: 340 mg (82%). Anal. Calcd for $C_{18}H_{13}N_2OClPd$ (%): C, 52.07; H, 3.16; N, 6.75. Found (%): C, 52.21; H, 3.09; N, 6.87. HRMS in $CHCl_3$-MeCN (1:1) m/z found (calcd) for $[M–Cl+MeCN]^+$: 420.0407 (420.0328). Selected IR bands: ν (cm^{-1}) = 3178 (N–H), 1612 (C=O), 1596 (C=N). UV-Vis in Me_2NCHO: λ_{max} (nm) (ε (10^4 M^{-1} cm^{-1})) = 442 (0.44), 419^{sh} (0.57), 394 (1.21), 374 (1.17), 356 (0.95). ^{1}H NMR in $(CD_3)_2SO$: δ (ppm) = 12.32 (br s, 1H), 8.85 (s, 1H), 8.33 (s, 1H), 8.11–7.99 (m, 2H), 7.83–7.33 (m, 6H), 7.25–7.16 (m, 1H), 7.01–6.94 (m, 1H).

*2.5. Synthesis of [Pd(L)(PPh_3)] (**2**)*

Solid PPh_3 (263 mg, 1 mmol) was added to a suspension of [Pd(HL)Cl] (**1**) (208 mg, 0.5 mmol) in acetone (25 ml) and the mixture was stirred at room temperature (298 K) for 24 h. The light yellow solid precipitated was collected by filtration, washed with acetone (2 x 10 ml) and finally dried in air. Yield: (230 mg, 72%). Anal. Calcd for $C_{36}H_{27}N_2OPPd$ (%): C,

67.45; H, 4.25; N, 4.37. Found (%): C, 67.31; H, 4.18; N, 4.46. HRMS in $CHCl_3$ m/z found (calcd) for $[M+H]^+$: 641.0971 (641.0974). Selected IR bands: ν (cm^{-1}) = 1587 (C=N). UV-Vis in Me_2NCHO: λ_{max} (nm) (ε (10^4 M^{-1} cm^{-1})) = 448 (0.63), 422 (0.78), 393 (1.26), 374 (1.18), 357 (0.84). ^1H NMR in $CDCl_3$: δ(ppm) (J (Hz)) = 8.04 (s, 1H), 8.02 (s, 1H), 7.91 (7) (d, 1H), 7.79–7.75 (m, 6H), 7.59 (6) (d, 1H), 7.56–7.52 (m, 4H), 7.49–7.46 (m, 6H), 7.42 (6) (d, 1H), 7.37 (6) (t, 2H), 7.26 (6) (t, 1H), 7.19 (6) (t, 1H), 6.80 (6) (d, 1H), 6.32 (3) (d, 1H). $^{31}P\{^1H\}$ NMR in $CDCl_3$: δ(ppm) = 34.06.

2.6. General procedure for double cross-coupling reactions

In a 10 ml round bottom flask, 3,5-dihalosalicylaldehyde (1 mmol), arylboronic acid (2.2 mmol for diiodo precursor or 2.5 mmol for dibromo precursor), $LiOH\cdot H_2O$ (2 mmol) and complex **2** (0.01 mol% for diiodo precursor or 0.05 mol% for dibromo precursor) in 0.1 ml dimethylformamide were taken in 2 ml of water-methanol (1:1) mixture. The reaction mixture was then heated at 80 °C under aerobic condition. Progress of the reaction was monitored by TLC. On completion, the reaction mixture was cooled to room temperature and extracted with two 10 ml portions of ethyl acetate. The combined extract was washed with water (2 x 10 ml), dried over anhydrous Na_2SO_4 and finally the solvent was removed under reduced pressure. The solid obtained was subjected to column chromatography over silica gel using ethyl acetate and hexane mixture as the eluent to afford the pure product. All the functionalized triaryl products obtained were characterized by ^1H-NMR spectroscopy and high resolution mass spectrometry.

2.7. X-ray crystallography

Single crystals of [Pd(HL)Cl] (**1**) were grown by diethyl ether vapor diffusion into its dimethylformamide solution, whereas single crystals of $[Pd(L)(PPh_3)]$ (**2)** were obtained by slow evaporation of its chloroform-methanol (1:1) solution. **1** crystallizes as **1**$\cdot Me_2NCHO$ and **2** crystallizes as it is without any solvent molecule. Unit cell determination and intensity data collection for **1**$\cdot Me_2NCHO$ were performed on an Oxford Diffraction Xcalibur Gemini single crystal X-ray diffractometer using graphite monochromated Mo $K\alpha$ radiation (λ = 0.71073 Å) at 298 K. Data collection, reduction and absorption correction were performed using the CrysAlisPro software [22]. In the case of **2**, a Bruker D8 QUEST diffractometer equipped with a PHOTON 100 CMOS area detector and an INCOATEC microfocus source for graphite-monochromated Mo $K\alpha$ radiation (λ = 0.71073 Å) was used for determination of

the unit cell and intensity data collection at 298 K. The APEX3 software package [23] was used for data collection, data integration, reduction and absorption correction. The structures of both complexes were solved by direct method and refined on F^2 by full-matrix least-squares procedures. The structure of **2** was refined as an inversion twin using the TWIN/BASF procedure [24]. The non-hydrogen atoms of both structures were refined anisotropically. In the case of **2**, four carbon atoms (two from benzoyl phenyl ring and two from PPh_3 phenyl ring) were refined with restraints on anisotropic displacement parameters. All hydrogen atoms were included in the structure factor calculation at idealized positions using a riding model. The SHELX-97 programs [24] available in the WinGX software suite [25] were used for structure solution and refinement. The Mercury package [26] was used to prepare the molecular illustrations. Selected crystallographic data are listed in Table S1 (Supplementary material).

3. Results and discussion

3.1. Synthesis and some properties

The Schiff base *N'*-(2-naphthaldimine)benzohydrazide (H_2L) was prepared in good yield (86%) by condensation reaction of equimolar amounts of 2-naphthaldehyde and benzohydrazide in methanol in presence of a few drops of acetic acid. The purity and the identity of H_2L have been confirmed by elemental analysis, mass spectrometric and spectroscopic (IR, UV-Vis and ^{1}H NMR) measurements. The palladium(II) complex [Pd(HL)Cl] (**1**) was synthesized in 77% yield by reacting in situ generated Li_2PdCl_4, $NaOAc{\cdot}3H_2O$ and H_2L in 1:1:1 mole ratio in methanol at room temperature. The second complex [Pd(L)(PPh_3)] (**2**) was synthesized in 73% yield by treating **1** with two equivalents of PPh_3 in acetone (Scheme 1). The excess PPh_3 is expected to facilitate the deprotonation of the amide functionality of HL^- in **1**. The elemental analyses data of **1** and **2** are in good agreement with their corresponding molecular formulas. In chloroform and dichloromethane, **2** is highly soluble but **1** is sparingly soluble. Both complexes are highly soluble in dimethylformamide and dimethylsulfoxide, sparingly soluble in acetonitrile and methanol and insoluble in hexane and toluene. Due to solvent restrictions and the solubility problem the positive ion ESI mass spectrum of **1** was collected in $CHCl_3$-MeCN (1:1) mixture, where its solubility is slightly better when compared with that in the pure solvents. The spectrum shows the base peak at 420.0407 corresponding to the cation where the chloride is replaced

by acetonitrile, i.e., [**1**–Cl+MeCN]$^+$. On the other hand, the spectrum of **2** in pure $CHCl_3$ displays the usual [**2**+H]$^+$ as the base peak at 641.0971. As expected for square-planar complexes of palladium(II), both **1** and **2** are diamagnetic. The electrically non-conducting nature of **1** and **2** in solution is consistent with their molecular formulas as neutral species.

3.2. X-ray molecular structures

The structures of **1**·Me_2NCHO and **2** have been solved in the monoclinic space groups *C*2/c and $P2_1$, respectively. The asymmetric unit of **1**·Me_2NCHO consists of one molecule each of the complex and the solvent dimethylformamide, while that of **2** contains two complex molecules. In **1**·Me_2NCHO, the solvent molecule is hydrogen bonded with the complex molecule. The structure of the solvated species is illustrated in Fig. 1. The O-atom of the solvent molecule and the amide-NH of the ligand HL^- are involved in this hydrogen bonding. The N(2)···O(2) distance and the N(2)–H···O(2) angle are 2.734(5) Å and 165°, respectively. In contrast, there is no significant interaction between the two complex molecules present in the asymmetric unit of **2**. Both molecules are very similar with respect to intramolecular bond lengths and bond angles. Thus the structure of one of these two independent molecules of **2** is depicted in Fig. 2. Selected bond parameters for **1**·Me_2NCHO and **2** are listed in Table 1. In each complex, the tridentate ligand (HL^- in **1** and L^{2-} in **2**) acts as pincer-like CNO-donor and forms fused 5,5-membered chelate rings. The structures reveal that the 2-naphthyl fragment of each of HL^- and L^{2-} is palladated at the 3-position instead of the 1-position. There are very few reports on cyclometallated 2-naphthyl containing chelating ligands [27–30]. As observed in the present study, generally 3-position gets regioselectively metallated when both 1- and 3-positions of the 2-naphthyl fragment are available [27–29]. In such cases, it is thought that the 1-position is not accessible for metallation due to steric hindrance caused by the H-atom at the *peri*-C (8-position). However, it has been shown that the 1-position of the 2-naphthyl group can be metallated when the 3-position is blocked by a substituent [30]. In the amide functionality (–C(=O)NH–) of HL^- in **1**, the C(12)–N(2) and the C(12)–O(1) bond lengths are 1.358 (5) and 1.246 (5) Å, respectively. These values are consistent with the neutral keto form of the amide functionality [13–15,17,19]. On the other hand, for **2** the average of C(12/12′)–N(2/2′) bond lengths and that of C(12/12′)–O(1/1′) bond lengths are 1.335(6) and 1.285(6) Å, respectively (Table 1). The shorter C(12/12′)–N(2/2′) and longer C(12/12′)–O(1/1′) bond lengths in **2** compared to the corresponding bond lengths

in **1** clearly indicate that the amide functionality of L^{2-} in **2** is deprotonated and their values suggest that the negative charge is delocalized over the amidate fragment [11–17,19,20]. The HL^- and the chloride constitute a CNOCl square-plane around the metal center in **1**, while the L^{2-} and the PPh_3 assemble a square-planar CNOP coordination environment for the metal center in **2**. In both complexes, the metal center has no deviation from the square-plane formed by the four coordinating atoms. The rms deviations from the mean plane constituted by the metal and the four coordinating atoms are within 0.01–0.02 Å. The amidate-O is expected to be a better σ-donor than the amide-O. As a consequence, the Pd–O(amidate) bond length in **2** is significantly shorter (by ~0.1 Å) than the Pd–O(amide) bond length in **1**. In contrast, the Pd–C bond length in **1** is shorter by ~0.05 Å than that in **2**. This lengthening of the Pd–C bond in **2** is very likely due to the better *trans*-directing ability of the amidate-O than the amide-O (Figs. 1 and 2). Similarly the stronger *trans*-effect of PPh_3 than Cl^- causes a longer (by ~0.02 Å) Pd–N(azomethine) bond length in **2** compared to that in **1** (Table 1). Overall, all the bond lengths and the bond angles associated with the metal centers in **1** and **2** are within the ranges observed for palladium(II) complexes with similar ligands [11,13–15,17,19].

3.3. Spectroscopic properties

Infrared spectra of the Schiff base (H_2L) and the complexes (**1** and **2**) were recorded by employing KBr pellets in the range 4000–400 cm^{-1}. A large number of bands have been observed in each of the three spectra. Except for few characteristic bands we have not attempted to assign the remaining bands. The free Schiff base (H_2L) displays the typical bands for the amide N–H and C=O stretching vibrations at 3199 and 1638 cm^{-1}, respectively. A medium intensity band observed at 1605 cm^{-1} has been assigned to the azomethine C=N stretching vibration. The spectrum of **1** displays the amide N–H stretch at 3178 cm^{-1}. Two medium intensity bands observed at 1612 and 1596 cm^{-1} are assigned to the amide C=O and the azomethine C=N stretching frequencies, respectively. Appearance of these two bands at lower frequencies compared to those of the free Schiff base is consistent with the coordination of both amide-O and azomethine-N to the metal center in **1**. On the other hand, the spectrum of **2** does not display the amide N–H and C=O stretching bands due to deprotonation of the amide functionality. A strong band observed at 1587 cm^{-1} is most likely associated with the one end coordinated diazine (C=N–N=C) like fragment of L^{2-} in **2**.

Electronic absorption spectra of H_2L, **1** and **2** were recorded in dimethylformamide. The spectrum of H_2L displays a broad band centered at 315 nm preceded by a couple of shoulders and followed by a relatively narrow band at 282 nm and a shoulder (Fig. S1, Supplementary material). This type of spectral profile is typical of organic compounds containing naphthyl group [15,31,32]. Pure naphthalene is known to display similar absorptions at higher energy region with more pronounced vibrational structure [33,34]. The spectral profile of naphthalene consists of a group of absorption bands centered at ~275 nm. The absorption profiles of the two complexes **1** and **2** are very similar to that of the naphthalene except for a large red-shift. A group of five bands are observed in the range 448–356 nm for both **1** and **2**. The spectrum of **2** is illustrated in Fig. S1 (Supplementary material). Thus the absorption bands observed for H_2L as well as its complexes **1** and **2** are due to transitions predominantly centered at their corresponding 2-naphthyl fragments.

^{1}H NMR spectra of H_2L and **1** were recorded in $(CD_3)_2SO$ solution and the ^{1}H and $^{31}P\{^1H\}$ spectra of **2** were recorded in $CDCl_3$ solution. The amide N–H proton of H_2L resonates as a singlet at δ 11.99 ppm. The azomethine proton and the proton at the 1-position of the 2-naphthyl fragment of H_2L appear as two one-proton singlets at δ 8.64 and 8.16 ppm, respectively. The remaining aromatic protons are observed as a six-proton multiplet and another five-proton multiplet having the chemical shifts centered at δ ~7.98 and ~7.58 ppm, respectively. A broad singlet at δ 12.32 ppm due to the amide N–H proton of the ligand HL^- is observed in the spectrum of **1**. As in the free Schiff base, here also two one-proton singlets corresponding to the azomethine proton and the proton at the 1-position of the 2-naphthyl fragment of HL^- are observed at δ 8.85 and 8.33 ppm, respectively. Slight downfield shifts of these three resonances in **1** when compared with those in free H_2L are not unusual considering the deshielding caused by coordination of the amide-O and the azomethine-N to the palladium(II) center. The remaining ten aromatic protons belonging to the 2-naphthyl and the phenyl rings of HL^- appear as four multiplets centered at δ ~8.05, ~7.58, ~7.21 and ~6.98 ppm. As expected the spectrum of **2** does not display the signal corresponding to the amide N–H due to deprotonation. The spectrum shows two closely spaced one-proton singlets at δ 8.04 and 8.02 ppm followed by a one-proton doublet at δ 7.91 ppm. The singlets are very likely to be due to the protons at the 1- and 4-positions of the 2-naphthyl fragment of L^{2-}. The one-proton doublet is assigned to the azomethine proton. The doublet splitting is attributed to

the PPh_3 P-atom coordinated at the *trans*-position with respect to the azomethine-N. There is a significant upfield shift of the azomethine proton in **2** compared to that in H_2L and **1**. It is very likely that the stronger σ-donor PPh_3 facilitates better π-backdonation from metal to azomethine in **2** and hence causes the upfield shift of the azomethine proton. The remaining nine aromatic protons of L^{2-} and fifteen protons of the PPh_3 phenyl rings appear in the range δ 7.79–6.32 ppm with various splitting patterns such as doublet, triplet and multiplet. In general, the aromatic protons in the complexes are observed over a broader chemical shift range than in the free Schiff base due to shielding/deshielding caused by metal coordination and presence of the monodentate ancillary ligands. The singlet observed at δ 34.06 ppm in the $^{31}P\{^1H\}$ NMR spectrum of **2** confirms the presence of PPh_3 as the ancillary ligand.

3.4. Catalysis studies

Functionalized polyaryls and polyheteroaryls are of considerable interest because of their potential applications in natural products, biological, agrochemical, pharmaceutical and materials research [35–39]. Hence, there has been a continuous effort to develop new and efficient methods for the synthesis of such species [40–43]. Among the various strategies used so far, the simplest and most versatile approach is the palladium catalyzed Suzuki-Miyaura poly cross-coupling reactions of polyhaloaromatic compounds with arylboronic acids [44–47]. In the present work, we have attempted the one-pot synthesis of functionalized triaryls via double cross-coupling reactions of 3,5-dihalosalicylaldehydes with various arylboronic acids using the cyclopalladated complexes **1** and **2** as catalysts. The reaction of 3,5-diiodosalicylaldehyde and phenylboronic acid in presence of **2** as catalyst was chosen as the model reaction to screen the bases and the solvents (Table S2, Supplementary Material). Among the various inorganic bases used in water-methanol (1:1) as the reaction solvent (entries 1–6), $LiOH\cdot H_2O$ was found to provide the best yield (94 %) of the double cross-coupling product 3,5-diphenylsalicylaldehyde at a reaction temperature of 80 °C (entry 4). No coupling product was detected in the absence of base (entry 7). Using $LiOH\cdot H_2O$ as the base the reaction was then performed in various water-solvent (1:1) mixtures (entries 8–13). In all these reaction solvents, no yield to very poor yields were observed. Subsequently the reaction was conducted under the identical conditions as described in entry 4 except for the use of **1** instead of **2** as catalyst (entry 14). The change of the catalyst caused a significantly low yield (80%) of the coupled product and indicated that **2** is a better catalyst than **1**. Thus

the optimal reaction conditions were found to be the use of 3,5-diiodosalicylaldehyde (1 mmol), phenylboronic acid (2.2 mmol), $LiOH \cdot H_2O$ (2 mmol) and **2** (0.01 mol%) in water-methanol (1:1) at 80 °C for 15 h (entry 4).

To examine the substrate scope of the catalyst **2**, one-pot double cross-coupling reactions of 3,5-diiodosalicylaldehyde with various arylboronic acids were performed under the above mentioned optimal conditions. The results are summarized in Table 2. As observed with phenylboronic acid (entry 1), high yields (88–92%) of the double cross-coupled products were also obtained with *p*-methoxy-, *p*-fluoro-, and *m*-chlorophenylboronic acids and 2-naphthylboronic acid but in 5 to 9 h longer reaction times (entries 2–5). Comparatively rather low yield (74%) was obtained with *o*-anisolylboronic acid even in longer reaction duration (entry 6).

The scope of the catalyst **2** was further extended to double cross-coupling reactions of 3,5-dibromosalicylaldehyde with the same group of arylboronic acids which was used for 3,5-diiodosalicylaldehyde. The reaction of 3,5-dibromosalicylaldehyde with phenylboronic acid under the same optimal conditions described above for the diiodo precursor provided the product 3,5-diphenylsalicylaldehyde but in significantly low yield (40%). However, increase of the catalyst loading from 0.01 to 0.05 mol% and the amount of the phenylboronic acid doubled the yield to 82% in 24 h of reaction time (Table 3, entry 1). The reactions with the remaining arylboronic acids were then performed with the higher (0.05 mol%) catalyst loading and arylboronic acid to dibromo precursor mole ratio (2.5:1) (entries 2–6). The corresponding double cross-coupled products were isolated in moderate to good yields (60–83%). In general, despite the use of higher catalyst loading and mole ratio of the reactants and comparable or longer reaction times, the yields of the coupled products from the dibromo precursor are less (Table 3) than the yields obtained in the case of the diiodo precursor (Table 2). This difference in the reactivities is attributable to the fact that the C–Br bond is stronger than the C–I bond [48].

4. Conclusions

Synthesis, characterization and spectroscopic properties of the Schiff base *N′*-(2-naphthaldimine)benzohydrazide (H_2L) and the cyclometallated palladium(II) complexes [Pd(HL)Cl] and [Pd(L)(PPh_3)] with it have been described. The X-ray molecular structures of the two complexes demonstrate pincer-like CNO coordination mode of both HL^- and $L^{2-}$and

regioselective cyclopalladation at the 3-position of the 2-naphthyl group of each ligand. The spectroscopic characteristics of the two complexes are consistent with their molecular structures. Catalytic properties of both complexes in one-pot Suzuki-Miyaura double cross-coupling reactions of 3,5-dihalosalicylaldehydes with a variety of arylboronic acids have been investigated. Between the two complexes, [Pd(L)(PPh_3)] has been found to be the better perfoming catalyst . The catalytic reactions exhibited reasonable substrate scope and provided moderate to excellent yields of the functionalized triaryls.

Acknowledgements

G. N. Babu thanks the Council of Scientific and Industrial Research, New Delhi for a research fellowship (No. 09/414(1025)/2012-EMR-I). Financial and infrastructure supports from the University Grants Commission, New Delhi (through the UPE and CAS programs) and the Department of Science and Technology, New Delhi (through the PURSE and FIST programs) are gratefully acknowledged.

Appendix A. Supplementary material

CCDC 1553122 and 1553123 contain the supplementary crystallographic data for **1**·Me_2NCHO and **2**, respectively. These data can be obtained free of charge via www.ccdc.cam.ac.uk/data_request/cif, by e-mailing to data_request@ccdc.cam.ac.uk or by contacting The Cambridge Crystallographic Data Centre, 12 Union Road, Cambridge CB2 1EZ, UK; fax: (+44)1223-336-033. Supplementary Tables S1 and S2 and Fig. S1 related to this article can be found in the online version.

References

[1] G. Zhou, W.–Y. Wong, X. Yang, Chem. Asian J. 6 (2011) 1706–1727.

[2] C.–H. Siu, C.–L. Ho, J. He, T. Chen, P. Majumda, J. Zhao, H. Li, W.–Y. Wong, Polyhedron 82 (2014) 71–79.

[3] Y. You, W. Nam, Chem. Soc. Rev. 41 (2012) 7061–7084.

[4] Q. Zhao, C. Huang, F. Li, Chem. Soc. Rev. 40 (2011) 2508–2524.

[5] N. Cutillas, G.S. Yellol, C. de Haro, C. Vicente, V. Rodríguez, J. Ruiz, Coord. Chem. Rev. 257 (2013) 2784–2797.

[6] I. Omae, Coord. Chem. Rev. 280 (2014) 84–95.

[7] X. Jiang, N. Zhu, D. Zhao, Y. Ma, Sci. China Chem., 59 (2016) 40–52.

[8] L. Cuesta, E.P. Urriolabeitia, Comm. Inorg. Chem. 33 (2012) 55–85.

[9] K. Godula, D. Sames, Science 312 (2006) 67–72.

[10] Y.–F. Han, G.–X. Jin, Chem. Soc. Rev. 43 (2014) 2799–2823.

[11] S. Das, S. Pal, J. Organomet. Chem. 689 (2004) 352–360.

[12] R. Raveendran, S. Pal, J. Organomet. Chem. 692 (2007) 824–830.

[13] A.R.B. Rao, S. Pal, J. Organomet. Chem. 696 (2011) 2660–2664.

[14] A.R.B. Rao, S. Pal, J. Organomet. Chem. 701 (2012) 62–67.

[15] A.R.B. Rao, S. Pal, J. Organomet. Chem. 731 (2013) 67–72.

[16] K. Nagaraju, S. Pal, J. Organomet. Chem. 737 (2013) 7–11.

[17] A.R.B. Rao, S. Pal, J. Organomet. Chem. 762 (2014) 58–66.

[18] R.N. Prabhu, S. Pal, J. Chem. Sci. 127 (2015) 589–596.

[19] G.N. Babu, S. Pal, J. Organomet. Chem. 805 (2016) 19–26.

[20] G.N. Babu, S. Pal, J. Organomet. Chem. 824 (2016) 42–47.

[21] D.D. Perrin, W.L.F. Armarego, D.P. Perrin, Purification of Laboratory Chemicals, second ed., Pergamon, Oxford, 1983.

[22] CrysAlisPro Version 1.171.36.28, Agilent Technologies, Yarnton, Oxfordshire, UK, 2013.

[23] Bruker (2016). APEX3, SAINT-Plus and SADABS. Bruker AXS Inc., Madison, Wisconsin, USA.

[24] G.M. Sheldrick, Acta Crystallogr. Sect. A 64 (2008) 112–122.

[25] L.J. Farrugia, J. Appl. Crystallogr. 45 (2012) 849–854.

[26] F. Macrae, I.J. Bruno, J.A. Chisholm, P.R. Edgington, P. M. Cabe, E. Pidcock, L. Rodriguez-Monge, R. Taylor, J. van de Streek, P.A. Wood, J. Appl. Crystallogr. 41 (2008) 466–470.

[27] J.–M. Valk, F. Maassarani, P. van der Sluis, A.L. Spek, J. Boersma, G. van Koten, Organometallics 13 (1994) 2320–2329.

[28] M. Crespo, M. Font-Bardía, S. Pérez, X. Solans, J. Organomet. Chem. 642 (2002) 171–178.

[29] S. Fuertes, H. García, M. Perálvarez, W. Hertog, J. Carreras, V. Sicilia, Chem. Eur. J. 21 (2015) 1620–1631.

[30] J.–M. Valk, R. van Belzen, J. Boersma, A.L. Spek, G. van Koten, J. Chem. Soc. Dalton Trans. (1994) 2293–2302.

[31] J.R. Cardinal, P. Mukerjee, J. Phys. Chem. 82 (1978) 1614–1620.

[32] P.K. Lekha, T. Ghosh, E. Prasad, J. Chem. Sci. 123 (2011) 919–926.

[33] J.M. Dixon, M. Taniguchi, J.S. Lindsey, Photochem. Photobiol. 81 (2005) 212–213.

[34] J. Krausko, J.K. Malongwe, G. Bičanová, P. Klán, D. Nachtigallová, D. Heger, J. Phys. Chem. A 119 (2015) 8565−8578.

[35] J.–K. Liu, Chem. Rev. 106 (2006) 2209–2223.

[36] F. Bellina, R. Rossi, Tetrahedron 62 (2006) 7213–7256.

[37] G. Hervé, C. Len, Sust. Chem. Proc. 3 (2015) 3.

[38] J.E. Anthony, Chem. Rev. 106 (2006) 5028–5048.

[39] A.R. Murphy, J.M.J. Fréchet, Chem. Rev. 107 (2007) 1066–1096.

[40] D. Pérez, E. Guitián, Chem. Soc. Rev. 33 (2004) 274–283.

[41] X. Feng, W. Pisula, K. Müllen, Pure Appl. Chem. 81 (2009) 2203–2224.

[42] D. Pérez, D. Peña, E. Guitián, Eur. J. Org. Chem. (2013) 5981–6013.

[43] T. Truong, M. Mesgar, K.K.A. Le, O. Daugulis, J. Am. Chem. Soc. 136 (2014) 8568−8576.

[44] L. Liu, Y. Zhang, B. Xin, J. Org. Chem. 71 (2006) 3994–3997.

[45] F. Beaumard, P. Dauban, R. H. Dodd, Org. Lett. 11 (2009) 1801−1804.

[46] A.R. Chaudhary, A.V. Bedekar, Appl. Organometal. Chem. 26 (2012) 430–437.

[47] S. Reimann, P. Ehlers, M. Sharif, A. Spannenberg, P. Langer, Tetrahedron 72 (2016) 1083−1094.

[48] Y.–R. Luo, Handbook of Bond Dissociation Energies in Organic Compounds, CRC Press LLC, Boca Raton, 2003.

Table 1

Selected bond lengths (Å) and angles (°) for **1**·Me_2NCHO and **2**

[Pd(HL)Cl]·Me_2NCHO (**1**·Me_2NCHO)			
Pd(1)–C(3)	1.953(4)	Pd(1)–N(1)	1.977(3)
Pd(1)–O(1)	2.208(3)	Pd(1)–Cl(1)	2.2929(12)
C(12)–N(2)	1.358(5)	C(12)–O(1)	1.246(5)
C(3)–Pd(1)–N(1)	81.89(15)	C(3)–Pd(1)–O(1)	158.13(14)
C(3)–Pd(1)–Cl(1)	98.89(13)	N(1)–Pd(1)–O(1)	76.26(12)
N(1)–Pd(1)–Cl(1)	178.89(9)	O(1)–Pd(1)–Cl(1)	102.97(8)
[Pd(L)(PPh_3)] (**2**)			
Molecule 1			
Pd(1)–C(3)	2.008(5)	Pd(1)–N(1)	1.996(4)
Pd(1)–O(1)	2.107(3)	Pd(1)–P(1)	2.2594(11)
C(12)–N(2)	1.333(6)	C(12)–O(1)	1.288(6)
C(3)–Pd(1)–N(1)	82.25(18)	C(3)–Pd(1)–O(1)	158.52(15)
C(3)–Pd(1)–P(1)	98.94(13)	N(1)–Pd(1)–O(1)	76.40(15)
N(1)–Pd(1)–P(1)	178.55(13)	O(1)–Pd(1)–P(1)	102.38(10)
Molecule 2			
Pd(1′)–C(3′)	2.005(5)	Pd(1′)–N(1′)	2.002(4)
Pd(1′)–O(1′)	2.113(3)	Pd(1′)–P(1′)	2.2586(11)
C(12′)–N(2′)	1.337(6)	C(12′)–O(1′)	1.282(6)
C(3′)–Pd(1′)–N(1′)	82.62(19)	C(3′)–Pd(1′)–O(1′)	158.62(16)
C(3′)–Pd(1′)–P(1′)	98.61(15)	N(1′)–Pd(1′)–O(1′)	76.17(16)
N(1′)–Pd(1′)–P(1′)	178.18(14)	O(1′)–Pd(1′)–P(1′)	102.53(9)

Table 2

Reactions of 3,5-diiodosalicylaldehyde with arylboronic acids[a]

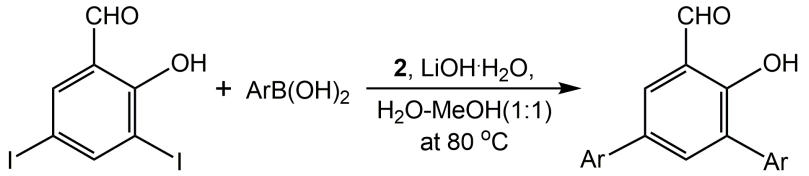

Entry	Ar	Time (h)	Yield[b] (%)
1	phenyl	15	94
2	*p*-anisolyl	24	88
3	*p*-fluorophenyl	20	90
4	*m*-chlorophenyl	24	92
5	2-naphthyl	24	90
6	*o*-anisolyl	24	74

[a] Conditions: 3,5-Diiodosalicylaldehyde (1 mmol), arylboronic acid (2.2 mmol), $LiOH \cdot H_2O$ (2 mmol), **2** (0.01 mol%) in 0.1 ml of dimethylformamide, H_2O-MeOH in 1:1 volume ratio (2 ml), 80 °C.

[b] Isolated yield.

Table 3

Reactions of 3,5-dibromosalicylaldehyde with arylboronic acids[a]

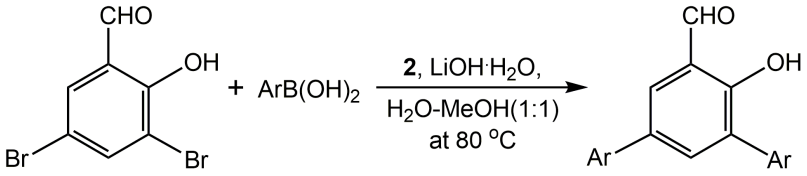

Entry	Ar	Time (h)	Yield[b] (%)
1	phenyl	24	82
2	*p*-anisolyl	24	80
3	*p*-fluorophenyl	24	84
4	*m*-chlorophenyl	30	60
5	2-naphthyl	30	62
6	*o*-anisolyl	24	83

[a] Conditions: 3,5-Dibromosalicylaldehyde (1 mmol), arylboronic acid (2.5 mmol), $LiOH \cdot H_2O$ (2 mmol), **2** (0.05 mol%) in 0.1 ml of dimethylformamide, H_2O-MeOH in 1:1 volume ratio (2 ml), 80 °C.

[b] Isolated yield.

Figure Captions

Scheme 1. Conversion of [Pd(HL)Cl] (**1**) to [Pd(L)(PPh_3)] (**2**).

Fig. 1. ORTEP representation of [Pd(HL)Cl]·Me_2NCHO (**1**·Me_2NCHO) with the atom numbering scheme. All non-hydrogen atoms are shown by their 50% probability thermal ellipsoids.

Fig. 2. ORTEP representation of one of the two molecules of [Pd(L)(PPh_3)] (**2**) present in the asymmetric unit. The thermal ellipsoids for the non-hydrogen atoms are drawn at the 50% probability level. All non-carbon atoms and a few selected carbon atoms are labeled for clarity.

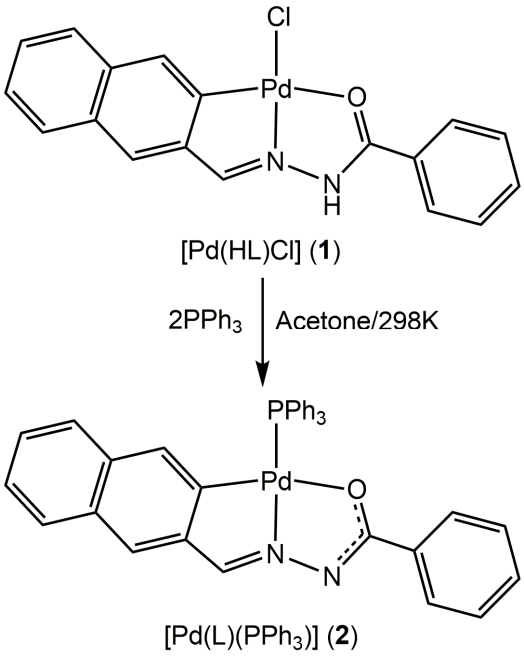

Scheme 1

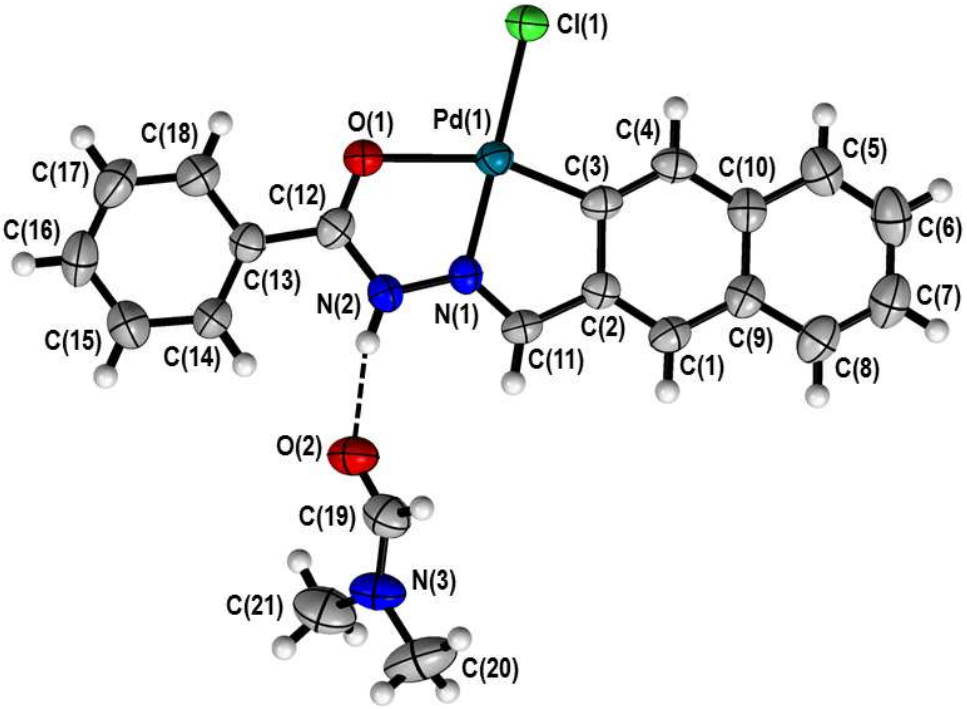

Figure 1

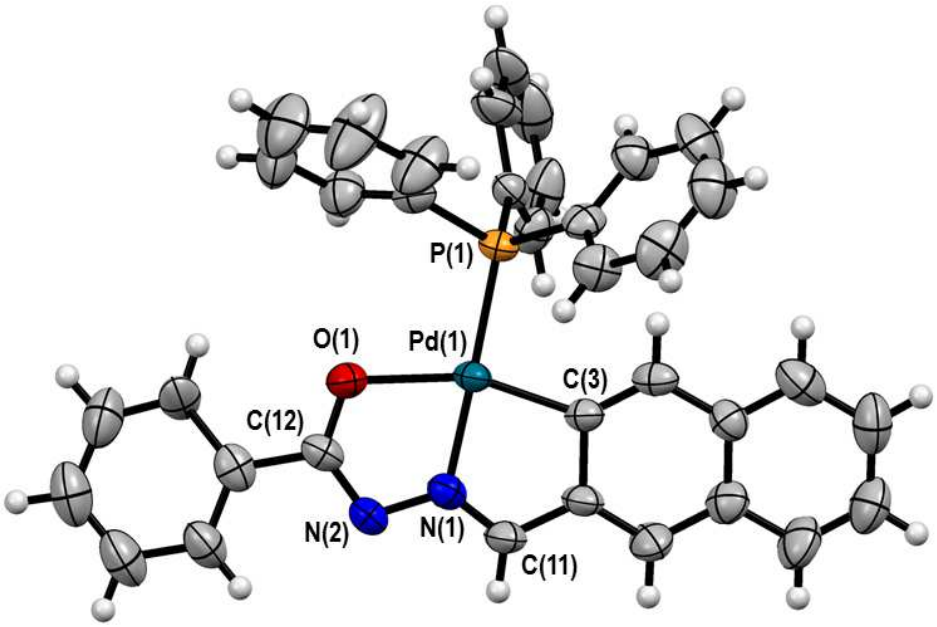

Figure 2

Research Highlights

- Cyclopalladation chemistry of *N*′-(2-naphthaldimine)benzohydrazide (H_2L) was examined.
- Mononuclear cyclopalladates [Pd(HL)Cl] and [Pd(L)(PPh_3)] were isolated.
- Structures of both complexes were studied by X-ray crystallography and spectroscopy.
- 2-naphthyl of each of HL^- and L^{2-} is regioselectively cyclometallated at 3-position.
- [Pd(L)(PPh_3)] efficiently catalyzed Suzuki-Miyaura double cross-coupling reactions.